Fracture Mechanics of Concrete Structures
Proceedings FRAMCOS-3
AEDIFICATIO Publishers, D-79104 Freiburg, Germany

DAMAGE ANALYSIS OF NOTCHED CONCRETE BEAMS LOADED IN FOUR-POINT-SHEAR

M.G.D. Geers
Faculty of Civil Engineering, Royal Military Academy,
Brussels, Belgium
R. de Borst
Faculty of Civil Engineering, Delft University of Technology,
Delft, The Netherlands
R.H.J. Peerlings
Faculty of Mechanical Engineering, Eindhoven University of Technology,
Eindhoven, The Netherlands

Abstract

In recent years, various numerical models have been proposed to analyse the damage evolution in concrete structures. The present contribution focuses on a gradient-enhanced damage formulation which is applied to single-edge-notched (SEN) and double-edge-notched (DEN) concrete beams loaded in four-point-shear. Experimentally observed curved crack paths, damage zones and splitting cracks are investigated through the use of freely rotating, fixed or constrained loading supports. The influence of the ratio of the compressive strength versus the tensile strength is scrutinized and its relation with the failure mechanism is investigated. A good agreement has been found between available experimental results and numerical simulations.

Key words: Gradient damage, four-point-shear, single-edge-notched beam, double-edge-notched beam, nonlocal.

1 Introduction

The past decades have shown a significant progress in the numerical modelling of concrete failure. This is typically the case where concrete is considered as a quasi-brittle material in which strain softening plays a dominant role. Many models have been proposed, following different approaches: fracture energy models, smeared crack models, Cosserat models, plasticity models, rate-dependent models, nonlocal damage models, gradient-enhanced models and others. An attractive approach is to include a nonlocal effect, e.g. nonlocal damage models and gradient damage or plasticity models (Pijaudier-Cabot et al., 1994; de Borst et al., 1995). These models solve the ill-posedness of the governing equations of the boundary value problem through the introduction of a microstructural characteristic, which is commonly denoted as an intrinsic length scale. In the present analysis, a gradient-enhanced damage formulation will be used to model failure of notched concrete beams.

Many authors have investigated the behaviour of concrete beams under mixed-mode loading conditions (Bažant and Pfeiffer, 1985; Ingraffea and Panthaki, 1985; Rots et al., 1987; Swartz and Taha, 1987; Carpinteri et al., 1989; Ferrara, 1991; Schlangen, 1993). Often, contradictory conclusions were drawn and different failure modes were recovered in the experimental analyses. The present simulations, which are based on the experiments carried out by Schlangen (1993), are carried out with freely rotating and fixed loading supports. It appeared that these boundary conditions (in the simulations and in the tests) have an important influence on the final failure mode, which explains experimentally observed differences in failure modes.

2 Gradient-enhanced damage for concrete fracture

Combination of an isotropic strain-based damage formulation with a gradient-enhanced damage evolution results in a damage model with an intrinsic length scale (Peerlings et al., 1996). The total stress-strain relation can be written as

$$\boldsymbol{\sigma} = (1-\omega)\,{}^{4}\boldsymbol{C} : \boldsymbol{\varepsilon} \tag{1}$$

with $\boldsymbol{\sigma}$ the Cauchy stress tensor, $\boldsymbol{\varepsilon}$ the infinitesimal strain tensor, ${}^{4}\boldsymbol{C}$ the fourth-order elastic stiffness tensor and ω the scalar-valued damage variable ($0 \leqslant \omega \leqslant 1$). The damage parameter ω is computed from the deformation history of the material through a monotonically increasing deformation history parameter κ, which equals the ultimate nonlocal equivalent strain $\bar{\varepsilon}_{eq}$ that the material has experienced in its loading history. This nonlocal characteristic is computed from the field of local equivalent strains ε_{eq} in

the vicinity of the material point via the following partial differential equation (Peerlings et al., 1996):

$$\bar{\varepsilon}_{eq} - c\,\nabla^2\bar{\varepsilon}_{eq} = \varepsilon_{eq} \tag{2}$$

This equation introduces a new material parameter c, the gradient parameter, which is related to the square of the intrinsic length scale of the nonlocal continuum. The solution of equation (2) requires the incorporation of appropriate boundary conditions (Peerlings et al., 1996).

An important aspect for concrete fracture resides in the precise definition of ε_{eq}, which has to be computed from the strain tensor $\boldsymbol{\varepsilon}$ in each material point. In the definition proposed by Peerlings et al. (1998), the relative contributions of the tensile and compressive strain components differ, which can have a major impact on the failure mode that is obtained. The equivalent strain definition used for concrete reads

$$\varepsilon_{eq} = \frac{k-1}{2k\,(1-2\nu)}J_1 + \frac{1}{2k}\sqrt{\left(\frac{k-1}{1-2\nu}J_1\right)^2 + \frac{6k}{(1+\nu)^2}J_2} \tag{3}$$

where the following strain tensor invariants have been used

$$J_1 = \mathrm{tr}(\boldsymbol{\varepsilon}) = \varepsilon_1 + \varepsilon_2 + \varepsilon_3$$

$$J_2 = \mathrm{tr}(\boldsymbol{\varepsilon}\cdot\boldsymbol{\varepsilon}) - \frac{1}{3}\mathrm{tr}^2(\boldsymbol{\varepsilon}) = \frac{1}{3}\left((\varepsilon_1-\varepsilon_2)^2 + (\varepsilon_2-\varepsilon_3)^2 + (\varepsilon_1-\varepsilon_3)^2\right)$$

In here, the parameter k controls the sensitivity to tensile and compressive strains ($k \approx f_{cc}/f_{ct}$).

The damage parameter ω is computed directly from a damage evolution law, which describes the mechanical influence of the material degradation. The used damage evolution law for concrete is

$$\omega = 1 - \frac{\kappa_i}{\kappa}\left[(1-\alpha) + \alpha e^{-\beta(\kappa-\kappa_i)}\right] \tag{4}$$

where the coefficients α and β are material parameters. More computational details can be found in Peerlings et al. (1996).

2.1 Beams loaded with freely rotating supports

2.1.1 Single-edge notched beam

The geometry and the loading conditions of the single-edge notched (SEN) beam are given in Fig. 1. The specimen is subjected to an antisymmetric four-point-shear loading.

The thickness of the bar equals 50 mm. The antisymmetric loading of the beam results in a curved crack path, which starts from the right corner of the

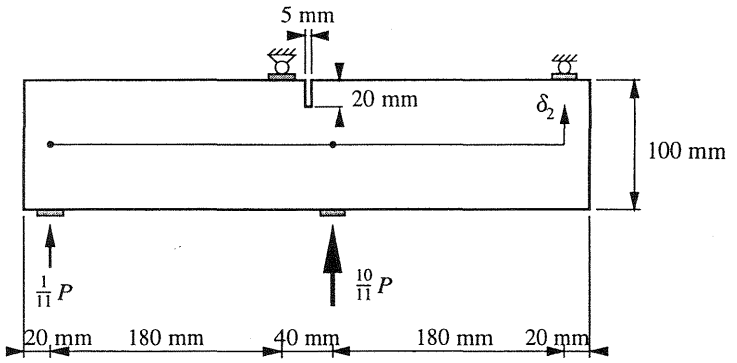

Fig. 1. Single-edge notched beam configuration

notch and which ends at the lower right loading platen. The beam has been modelled with 5x5 mm^2 eight-noded quadrilateral elements for the coarse mesh and 2.5x2.5 mm^2 elements for the fine mesh. The material parameters used in this model are: Young's modulus $E = 35000$ MPa, Poisson's ratio $\nu = 0.2$, gradient parameter $c = 1$ mm^2, compression-tension sensitivity $k = 15$, damage initiation history parameter $\kappa_i = 6.e-5$, damage evolution law parameters $\alpha = 0.96$ and $\beta = 100$.

Damage initiates at the right corner of the notch and at the bottom of the beam, opposite to the upper central loading platen. The damage growth at the bottom is arrested, while it keeps growing at the notch. The experimentally observed curved crack path at a certain loading level is well reproduced. The final damage distribution computed for the coarse mesh is given in Fig. 2, while the comparison with the experimentally observed crack paths is made for the fine mesh in Fig. 3. All observed cracks are

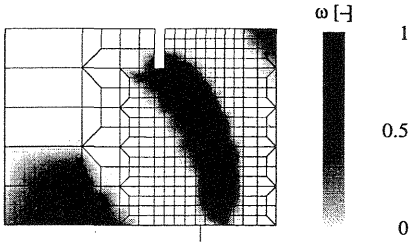

Fig. 2. Damage in coarse mesh

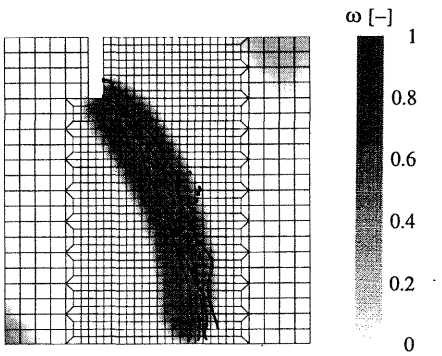

Fig. 3. Computed damage and experimental crack paths

located within the computed damage band. The secondary damage zones

at the opposite edge of the central loading platens have been confirmed experimentally. Fig. 4 shows the load P versus the crack mouth opening displacement (CMOD) for the simulation and the experiments, while Fig. 5 illustrates the mesh independence with respect to the load-CMSD (crack mouth sliding displacement) curves. The good quality of the simulation is

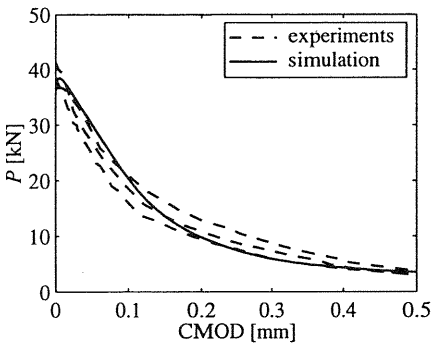

Fig. 4. P-CMOD curve

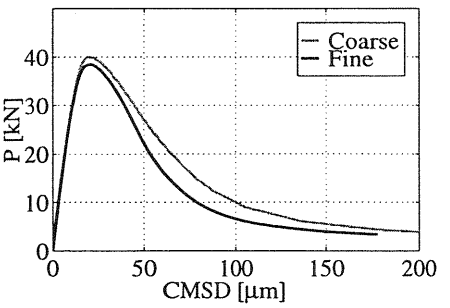

Fig. 5. Mesh independence

mainly attributable to the proper definition of the equivalent strain (3) which has been utilized in the numerical analysis.

2.1.2 Double-edge notched beam

The double-edge notched specimen, loaded in four-point-shear, is shown in Fig. 6. The loading platens are positioned adjacent to the notch, which results in a smaller shear zone than that observed in the SEN-test. Consequently, the load is applied close to the notch (10 mm) and failure by shearing towards the notch is a possible failure mode in the absence of friction in the supports. In the experiment, the support platens are subjected to rotational and translational friction. The inclusion of some frictional aspects in the FEM-model for the loading platens seems appropriate therefore. This frictional effect turns out to be particularly important for the DEN-beam with freely rotating supports. Small rotational springs can be added to the support platens or a small eccentricity of the loading force on the platen can be easily introduced, while the positioning of the platens remains unaffected. If friction is totally neglected an antisymmetric solution is found that consists of two curved cracks which originate from each notch. If the compression-tension sensitivity ratio k is smaller than 15, the beam fails by shearing and compression failure at the notches. However, by adding a small eccentricity to the loading force, the failure mode becomes asymmetric and remains stable. The damage evolution in the beam is depicted in Fig. 7 and in Fig. 8 for an eccentricity of 2.5 mm and 1 mm respectively.

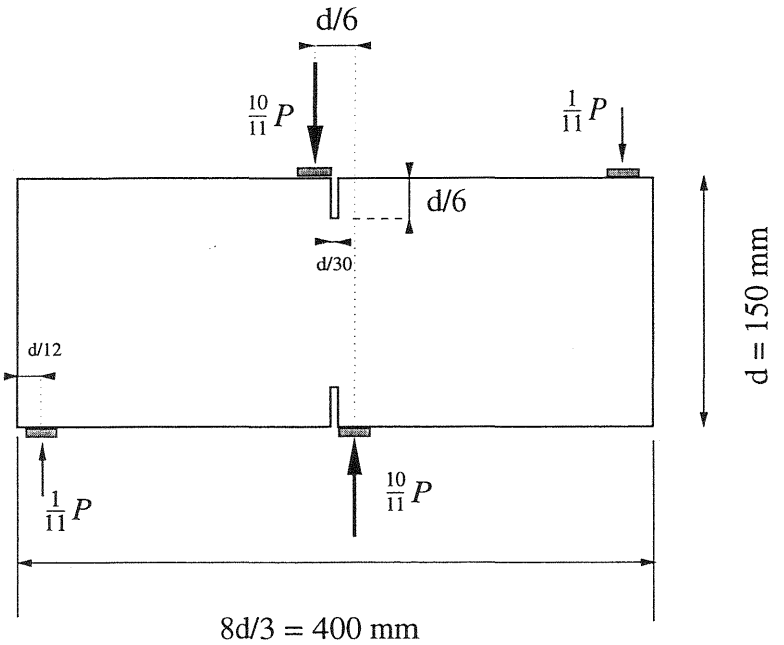

Fig. 6. Configuration of the DEN shear test.

A crack originates from each notch, but the lower crack is arrested, while the other crack continues to grow. The solution thus found corresponds well with the experimental solutions where a long crack and a short crack were found, see Fig. 9. It appears, that the length of the short crack depends on the eccentricity which was given to the loading point. For a smaller eccentricity, the second crack becomes longer (Fig. 7 and Fig. 8).

Other points of agreement are observed if the load-CMOD/CMSD curves of the simulations and the experiments are compared. It can be noticed from the numerical solution in Fig. 10 that larger eccentricities cause smaller maximum loads. This observation is confirmed by the experimental results in Fig. 11, where the numbers next to the curves correspond with the numbers indicated in Fig. 9. From this analysis, it may be concluded that small disturbances of the boundary conditions, which are inevitably present in an experiment, have an important influence on the final failure mode. These disturbances may be due to friction, but material heterogeneities in the vicinity of the loading platens are also possible.

2.2 Beams loaded with fixed supports

Schlangen (1993) carried out an experimental analysis on SEN and DEN-beams, using a fixed support loading system instead of freely rotating sup-

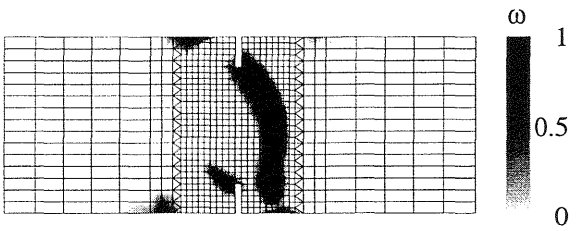

Fig. 7. Damage in DEN-beam with rotating supports, 2.5 mm eccentric load

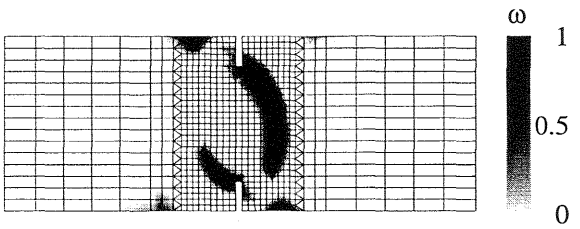

Fig. 8. Damage in DEN-beam with rotating supports, 1 mm eccentric load

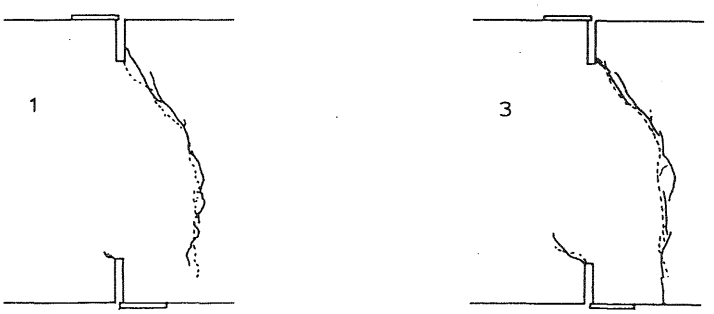

Fig. 9. Experimental crack patterns (Schlangen, 1993)

ports. The use of these constraints invariably introduces friction in the supports. These constraints were practically realized by mounting diagonal bars to the loading frame. Additional constraints were imposed on the rotations of the supports. In the FEM-model, the boundary conditions have to be modified accordingly. It is found that the applied boundary conditions which are used to model these constraints are important and may lead to different failure modes. To model the fixation of the supports linear constraints or spring elements were introduced in the FEM-model. However, it is not possible to give a complete quantitative analysis of the load-CMOD/CMSD results without taking into account the frictional effects in the supports, which have an important influence on measured forces and displacements.

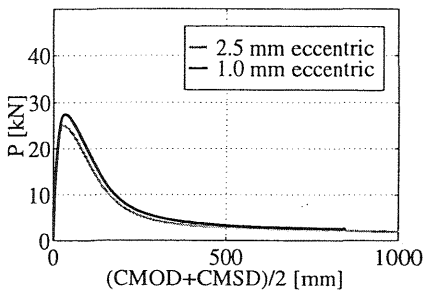

Fig. 10. Numerical results

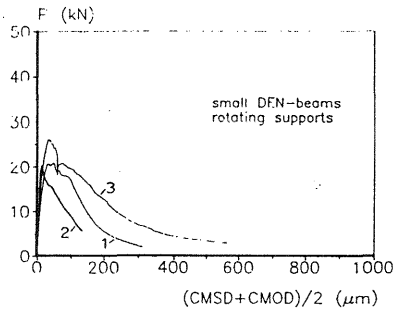

Fig. 11. Experiments (Schlangen, 1993)

The study is therefore limited to a qualitative interpretation of the computed failure modes and damage distributions.

2.2.1 Single-edge notched beam

The SEN-beam under fixed loading conditions is characterized by the appearance of a second flexural crack which starts at the unnotched side of the specimen as shown in the experimental crack pattern of Fig. 12. The fixed

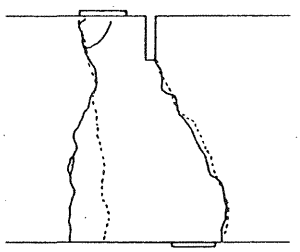

Fig. 12. Cracks in the SEN-beam with fixed supports (Schlangen, 1993)

loading frame was modelled with linear springs between the loaded nodes of interconnected loading platens combined with linear constraints in order to inhibit the free rotation of the platens. The failure mode shown in Fig. 13 is then obtained. The solution depends highly on the applied boundary conditions and of the stiffness on the constraining springs. If these springs are too stiff, a splitting crack is found at the centre of the beam, as depicted in Fig. 14.

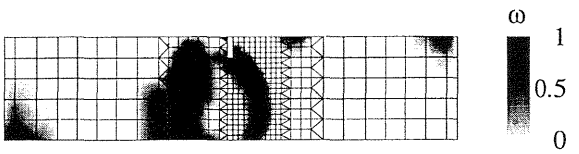

Fig. 13. Damage in SEN-beam with fixed supports.

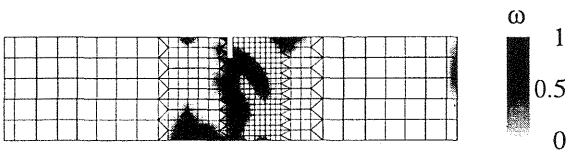

Fig. 14. Splitting crack in SEN-beam with fixed supports.

2.2.2 Double-edge notched beam

Several failure modes were found for the DEN-beam under fixed loading conditions. Experimentally, two failure patterns were observed which are shown in Fig. 15 and Fig. 16. Fig. 15 corresponds with an antisymmetric double curved crack mode, while Fig. 16 shows a splitting crack mode.

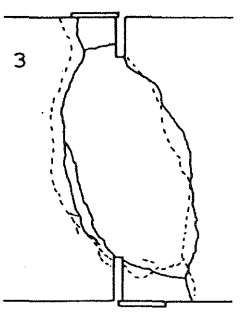

Fig. 15. DEN double curved crack mode (Schlangen, 1993)

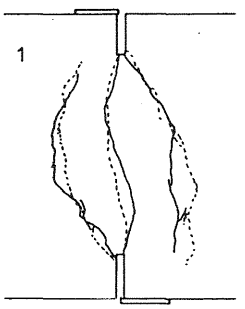

Fig. 16. DEN splitting crack mode (Schlangen, 1993)

In the experiment, cracks under the loading platens were only observed sporadically, while they are more prone to appear in a numerical simulation in which contact between concrete and loading platen cannot be described exactly. It may therefore be necessary to inhibit the failure in the vicinity of the loading platens which is due to the horizontal constraints. The fixed support loading frames were modelled with constraints between the two nodes of each loading frame. If the constraints are weak, e.g. due to some slip in the supports, or if significant damage occurs under the load-

ing platens, a double curved crack mode comes out naturally (Fig. 17). The cracks and damage in the neighbourhood of the supports can also be noticed in the experimental crack distribution shown in Fig. 15.

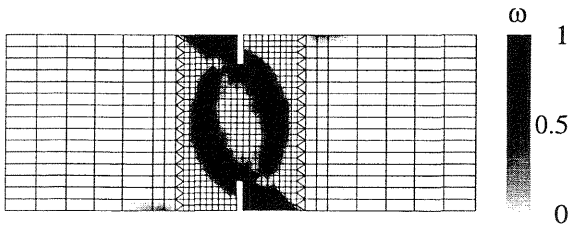

Fig. 17. Double curved damage zones in the DEN-beam with fixed supports.

Splitting cracks can be obtained by using a stiff loading frame and by inhibiting damage in the immediate vicinity of the platens. In this case, the double curved crack is arrested due to the horizontal forces in the specimen. The splitting crack arises at the centre of the beam, i.e. between the two other cracks. The development of the splitting crack is shown in Fig. 18 for a compression-tension sensitivity ratio k equal to 15. After the double

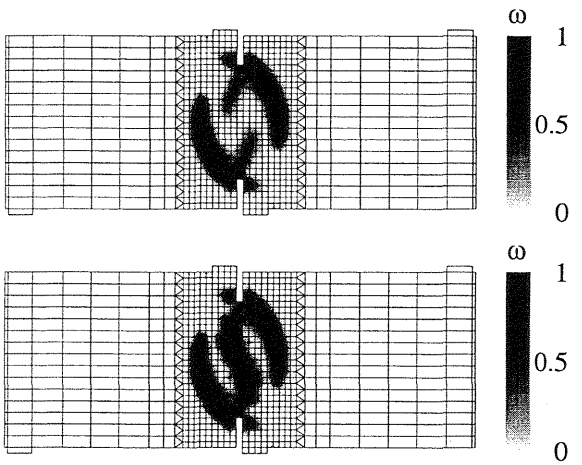

Fig. 18. Splitting crack in the DEN-beam with fixed supports.

curved crack has been arrested, the damage starts to grow near the notches and propagates towards the centre of the beam, which results in the characteristic S-shape of the splitting crack. The experimental S-shape is given in Fig. 16. All further damage then progresses from the centre of the beam, which results in the macroscopically observed splitting crack. On the other hand, if a smaller compression-tension sensitivity ratio k is applied, e.g. 10,

damage initiates from the centre of the beam instead of from the notches, as shown in Fig. 19. Obviously, the value of k has an important influence on the propagation of the crack and on the characteristic S-shape which is less pronounced for a smaller compression-tension sensitivity ratio.

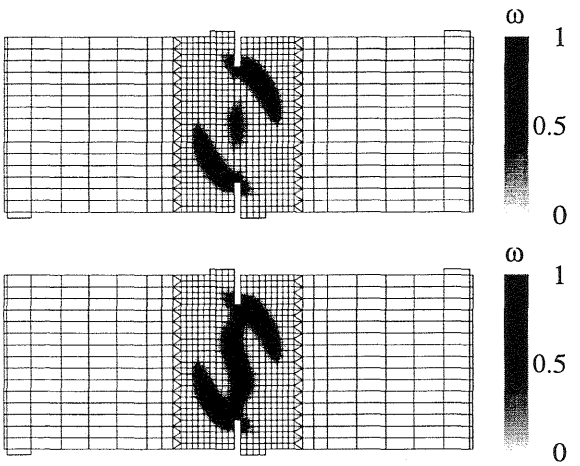

Fig. 19. Splitting crack in the fixed DEN-beam with k equal to 10.

3 Conclusions

Single-edge notched and double-edge notched concrete beams have been investigated numerically. A freely rotating and a fixed loading frame have been modelled with different boundary conditions. A gradient-enhanced damage model was used successfully to describe most of the experimentally observed phenomena: single curved cracks (SEN rotating), straight cracks (SEN fixed), asymmetric double curved cracks (DEN rotating), antisymmetric double curved cracks (DEN fixed) and splitting cracks with a characteristic S-shape (DEN fixed). The important influence of the boundary conditions in the loading supports on the final failure mode has been emphasized and the effect of the sensitivity to compressive strains versus tensile strains has been illustrated.

References

Bažant, Z. P. and Pfeiffer, P. A. (1985). Test of shear fracture and strain-softening in concrete. In **Proceedings of the 2nd Symposium of the Interaction of Non-Nuclear Munitions with Structures**, Panama City Beach, Florida.

Carpinteri, A., Ferrara, G. and Melchiorri, G. (1989). Single edge notched specimen subjected to four point shear: an experimental investigation. In **Fracture of Concrete and Rock - Recent Developments** (Eds. S. P. Shah, S. E. Swartz and B. Barr), 605–614. Elsevier Applied Science Publishers, London/New York.

de Borst, R., Pamin, J., Peerlings, R. H. J. and Sluys, L. J. (1995). On gradient-enhanced damage and plasticity models for failure in quasi-brittle and frictional materials. **Comp. Mech.**, 17, 130–141.

Ferrara, G. (1991). On the accuracy of the mixed mode tests performed at the enel-cris laboratories. Technical Report 4275, Enel-Cris, Milan, Italy.

Ingraffea, A. R. and Panthaki, M. J. (1985). Analysis of shear fracture tests of concrete beams. In **Finite Element Analysis of Reinforced Concrete Structures**, 151–173, Tokyo. ASCE.

Peerlings, R. H. J., de Borst, R., Brekelmans, W. A. M. and de Vree, J. H. P. (1996). Gradient-enhanced damage for quasi-brittle materials. **Int. J. Num. Meth. Eng.**, 39, 3391–3403.

Peerlings, R. H. J., de Borst, R., Brekelmans, W. A. M. and Geers, M. G. D. (1998). Gradient-Enhanced Damage Modelling of Concrete Fracture. **Mech. Coh.-Fric. Mat.** In press.

Pijaudier-Cabot, G., Dubé, J. F., Borderie, C. L. and Bodé, L. (1994). Damage models for concrete in transient dynamics. In **Fracture and Damage in Quasibrittle Structures - Experiment, modelling and computer analysis. Proceedings of the US-Europe Workshop** (Eds. Z. P. Bažant, Z. Bittnar, M. Jirásek and J. Mazars), 201–215, London. E & FN Spon.

Rots, J. G., Kusters, G. M. A. and Blauwendraad, J. (1987). Strain-softening simulations of mixed-mode concrete failure. In **Proceedings SEM/RILEM International Conference on Fracture of Concrete and Rock** (Eds. S. P. Shah and S. E. Swartz), 175–189, New York. Springer-Verlag.

Schlangen, E. (1993). **Experimental and numerical analysis of fracture processes in concrete**. Ph.D. thesis, Delft University of Technology.

Swartz, S. E. and Taha, N. (1987). Preleminary investigation of the suitability of the Iosipescu test specimen for determining mixed mode fracture properties of concrete. Technical Report 191, Kansas State University, Manhattan, Kansas.